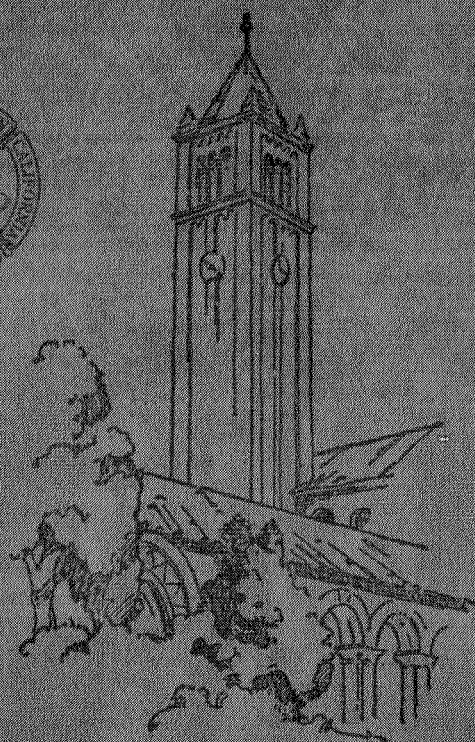
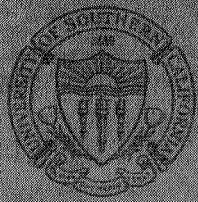


NASA CR 197043



CASE FILE COPY

THE MEASUREMENT OF OPTICAL CONSTANTS  
 IN THE VACUUM UV REGION, A FINAL  
 TECHNICAL REPORT

by

G. L. Weissler  
 Chief Investigator

NASA Grant No. NsG-178-61

DEPARTMENT OF PHYSICS  
 University of Southern California  
 Los Angeles, California 90007

Technical Report No. : USC-VacUV-119

15 October 1969

Contract NsG-178-61

on

VACUUM ULTRAVIOLET AND SOLID STATE PHYSICS

(This report covers the period from

1 November 1961 to 30 June 1969)

THE MEASUREMENT OF OPTICAL CONSTANTS  
IN THE VACUUM UV REGION, A FINAL  
TECHNICAL REPORT

by

G. L. Weissler

Chief Investigator

NASA Grant No. NsG-178-61

prepared for the

Office of Grants and Research Contracts  
National Aeronautics and Space Administration  
Washington 25, D. C.

THE MEASUREMENT OF OPTICAL CONSTANTS  
IN THE VACUUM UV REGION, A FINAL REPORT

on work done under auspices  
of NASA Grant No. NsG-178-61  
during the period from 1 Nov. 1961  
to 30 June 1969

by

G. L. Weissler  
Chief Investigator  
Department of Physics  
University of Southern California  
Los Angeles, California 90007

INTRODUCTION

The subject of this research was aimed at the determination of optical constants, the index of refraction "n" and the extinction coefficient "k", for surfaces produced and maintained under conditions of ultra-high vacua. This means that adsorbed, absorbed, or oxide films can either be totally avoided during the measurements or they can at least be drastically reduced.

In all instances, "n" and "k" were calculated by making use of the Fresnel Equations which relate the experimentally determined optical reflectance ( $I_{\text{reflected}}/I_{\text{incident}}$ ) to the complex dielectric constant\* and therefore to "n" and "k" and the plasma frequency.

---

\* The general theoretical relationships between optical properties and the dielectric constant have been summarized in two published lecture series: in particular, see E. Burnstein, in "Dynamical Processes in Solid State Optics", 1966 Tokyo Summer Lectures in Theoretical Physics, Part I, ed. R. Kubo and H. Kamimura; W. A. Benjamin, Inc., New York: 1967; p. 1; and H. Ehrenreich, in "Proc. E. Fermi School of Physics", 1965, Course XXXIV on "The Optical Properties of Solids", ed. J. Tauc; Academic Press, New York: 1966; p. 106.

The progress of research done in this area is best summarized by the following chronological list of Technical Reports, Thesis, and Publications achieved under this Grant:

1. "Optical Constants of Metals in the Vacuum UV Region", W. Steinmann, E. I. Fisher, and G. L. Weissler, USC-Tech. Report dated 15 January 1964.
2. "An Apparatus for Measuring the Reflection, Transmission, and Photoelectron Yields of Thin Metallic Films in the Extreme UV", Boyd MacNaughton, M. S. Thesis, USC 1964; also Tech. Report dated February 15, 1964.
3. "Far Ultraviolet Response of Silicon P-N Junction Photodiodes", D. B. Medved, Electro-Optical Systems, Inc., W. F. Crevier, A. L. Morse, USC, Bull. Am. Phys. Soc. 9, 644 (1964) (01); see also USC Tech. Report No. USC-VacUV-101, 15 June 1965.
4. "Some Instrumentation Problems below 1000Å", G. L. Weissler, ICO Conf., Tokyo, September 2-8, 1964; Japan. J. Appl. Phys. 4 (Supplement I), 486 (1965).
5. "A Rapidly Operating Vacuum Spark Source for the Vacuum Ultraviolet Region", (in French), G. Balloffett, J. Physique 25, 73A (1964).
6. "Optical Constants and Photoelectric Yields in the Soft X-Ray Region", G. L. Weissler, invited paper to the "Int'l. Conf. on the Physics of X-Rays", Cornell Univ., June 22-24, 1965; Bull. Am. Phys. Soc. 10, 1224 (1965).
7. "Optical Constants of Barium and Silver in the Vacuum Ultraviolet", E. I. Fisher, I. Fujita, and G. L. Weissler, J. Opt. Soc. Am. 56, 1560 (1966); see also Tech. Report No. USC-VacUV-108, dated 1 May 1966, by the same title.

8. "Photoemission from Al Films in the Extreme Ultraviolet", A. L. Morse and J. E. Rudisill, Bull. Am. Phys. Soc. 10, 1186 (1965) (A).
9. "Light Sources and Detectors for Work in the Vacuum Ultraviolet Region of the Spectrum", G. L. Weissler in "Aerospace Measurement Techniques", ed. G. G. Manella, pages 229-261, NASA SP-132, U.S. Government Printing Office, Washington: 1967.
10. "The Efficiency of Concave Gratings in the Extreme Ultraviolet", A. L. Morse and G. L. Weissler, Sci. Light (Tokyo) 15, 22 (1966).
11. "Photoemission Processes in Au and Al in the Extreme UV", A. L. Morse, Bull. Am. Phys. Soc. 13, 196 (1968).
12. "Optical and Photoelectric Properties, Including Polarization Effects, of Gold and Aluminum in the Extreme Ultraviolet", A. L. Morse, Dissertation, Univ. of So. Calif. 1967; also Tech. Report No. USC-VacUV-109 by same title, 5 January 1968.
13. "The Combination of an Ultrahigh Vacuum Seya Monochromator with an Ultrahigh Vacuum Reflectometer for Measurement of the Optical Constants of Solids in the Extreme UV", Hayden H. Bower, M. S. Thesis, Univ. of So. Calif., January 1969.

Since our research efforts from June 1967 to 30 June 1969 have only been covered in the semi-annual status reports and not in the detail of a Technical Report, it seems appropriate to do so in this Final Report. The following is taken from the M. S. thesis of Hayden H. Bower, listed under 13) above.

In conclusion, we would like to thank NASA for its financial assistance during this period and for the many encouragements given by the NASA monitors to our researchers.

THE COMBINATION OF AN ULTRAHIGH VACUUM SEYA MONOCHROMATOR  
WITH AN ULTRAHIGH VACUUM REFLECTOMETER FOR MEASUREMENT  
OF THE OPTICAL CONSTANTS OF SOLIDS IN THE EXTREME UV

by

Hayden H. Bower

---

A Thesis Presented To The  
FACULTY OF THE GRADUATE SCHOOL  
UNIVERSITY OF SOUTHERN CALIFORNIA  
In Partial Fulfillment of the  
Requirements for the Degree  
MASTER OF SCIENCE  
(Physics)

January 1969

## Table of Contents

Chapter	Page
I. Introduction.....	1
II. Experimental Apparatus.....	5
III. Reflectometer Evacuation.....	16
IV. Physical Measurements.....	23
V. Summary and Conclusion.....	31
List of References.....	32

## List of Figures

Figure	Page
1. Optical Arrangement.....	6
2. Ultrahigh Vacuum Monochromator.....	8
3. Angle Doubler Arrangement for Reflectance Measurements.....	11
4. Reflectometer Vacuum System.....	15
5. Ion Current vs. Nude Bayard-Alpert Pressure for Many Runs..	20
6. Ion Current vs. Nude Bayard-Alpert Pressure for One Run....	21
7. Reflectometer Target Design.....	25
8. Polarization Analyser.....	28



## Introduction

In recent years there has been considerable interest in determining the optical properties of various solids in the ultraviolet part of the spectrum, and investigations in the region between 200Å and 1000Å have become possible with the development of improved ultra-high vacuum equipment, light sources and detectors. The data gathered from these investigations provide a valuable means of checking the validity of current theories of optical absorption phenomena of solids.<sup>1</sup>

This work is concerned with the experimental determination of the optical constants and the energy loss functions for solids by measuring the reflectance,  $R$ , at different angles of incidence. The most common approach for thick films, where the thickness is larger than the wavelength of the radiation, in the desired wavelength region involves a solution of the Fresnel reflection equations<sup>2</sup> for the complex refractive index  $\tilde{n} = n - ik$ , where  $n$  is the ordinary index of refraction defined by

$$n = \frac{c}{v} ,$$

and  $k$  is the extinction coefficient. The absorption coefficient,  $\mu$ , in the Lambert-Beer law,

$$I = I_0 e^{-\mu z},$$

is related to this extinction coefficient by

$$\mu = \frac{4\pi k}{\lambda}.$$

The Fresnel equations express the total reflectance,  $R$ , as a function of the angle of incidence,  $\phi$ , the polarization of the incident beam,  $P$ , and the real and imaginary parts of  $\tilde{n}$ , where  $R$  is given by the ratio of the reflected intensity over the incident intensity. By using the reflectance measured for two different angles and determining the polarization, these equations can be graphically inverted to solve for  $n$  and  $k$ .<sup>3</sup> The equations have the following form:

$$R = [g(\phi, n, k) (P+1) + (1-P)] f(\phi, n, k),$$

where the functions  $g$  and  $f$  are defined by

$$g(\phi, n, k) = \frac{(a - \sin\phi \tan\phi)^2 + b^2}{(a + \sin\phi \tan\phi)^2 + b^2},$$

and

$$f(\phi, n, k) = \frac{(a - \cos\phi)^2 + b^2}{(a + \cos\phi)^2 + b^2},$$

with the terms  $a$  and  $b$  given by

$$2a^2 = [(n^2 - k^2 - \sin^2\phi)^2 + 4n^2 k^2]^{\frac{1}{2}} + (n^2 - k^2 \sin^2\phi),$$

$$2b^2 = [(n^2 - k^2 - \sin^2\phi)^2 + 4n^2 k^2]^{\frac{1}{2}} - (n^2 - k^2 \sin^2\phi),$$

and

$$P = \frac{(I_p - I_s)}{(I_p + I_s)} .$$

The subscripts p and s refer to the components of the electric vector polarized parallel and perpendicular to the plane of incidence, respectively.

Once the optical constants n and k have been determined, it is a simple matter to evaluate the energy-loss functions for the material. This is accomplished using the relation

$$(\epsilon)^{\frac{1}{2}} = n - ik = \tilde{n}$$

and the theoretical results of Fröhlich and Pelzer<sup>4</sup> which predict that the function  $\text{Im}(1/\epsilon)$  will have a maximum at the energy of the loss. In analogy to the above theoretical work, Kanazawa<sup>5</sup> predicted the function  $\text{Im}(1/\epsilon+1)$  would have a maximum at the energy of the surface loss. These functions, in terms of the optical constants are

$$\text{Im}(1/\epsilon) = \frac{2nk}{(n^2 + k^2)^2} ,$$

and

$$\text{Im}(1/\epsilon+1) = \frac{2nk}{(n^2 + k^2 + 1)^2 - 4k^2} .$$

Many of the previous investigations, undertaken at conditions of ordinary high vacuum of  $10^{-5}$  to  $10^{-8}$  Torr, were hampered because the surfaces studied were contaminated and therefore not indicative

of the material's intrinsic properties. There are two ways the investigator may limit the effects of contamination. The first is to operate under ultrahigh vacuum conditions which affords the experimenter a sufficiently long time, before monolayer formation, to perform the measurement on an uncontaminated surface. The other involves sample preparation with procedures for maintaining sample purity varying according to the restrictions imposed by the chemical activity of the sample.

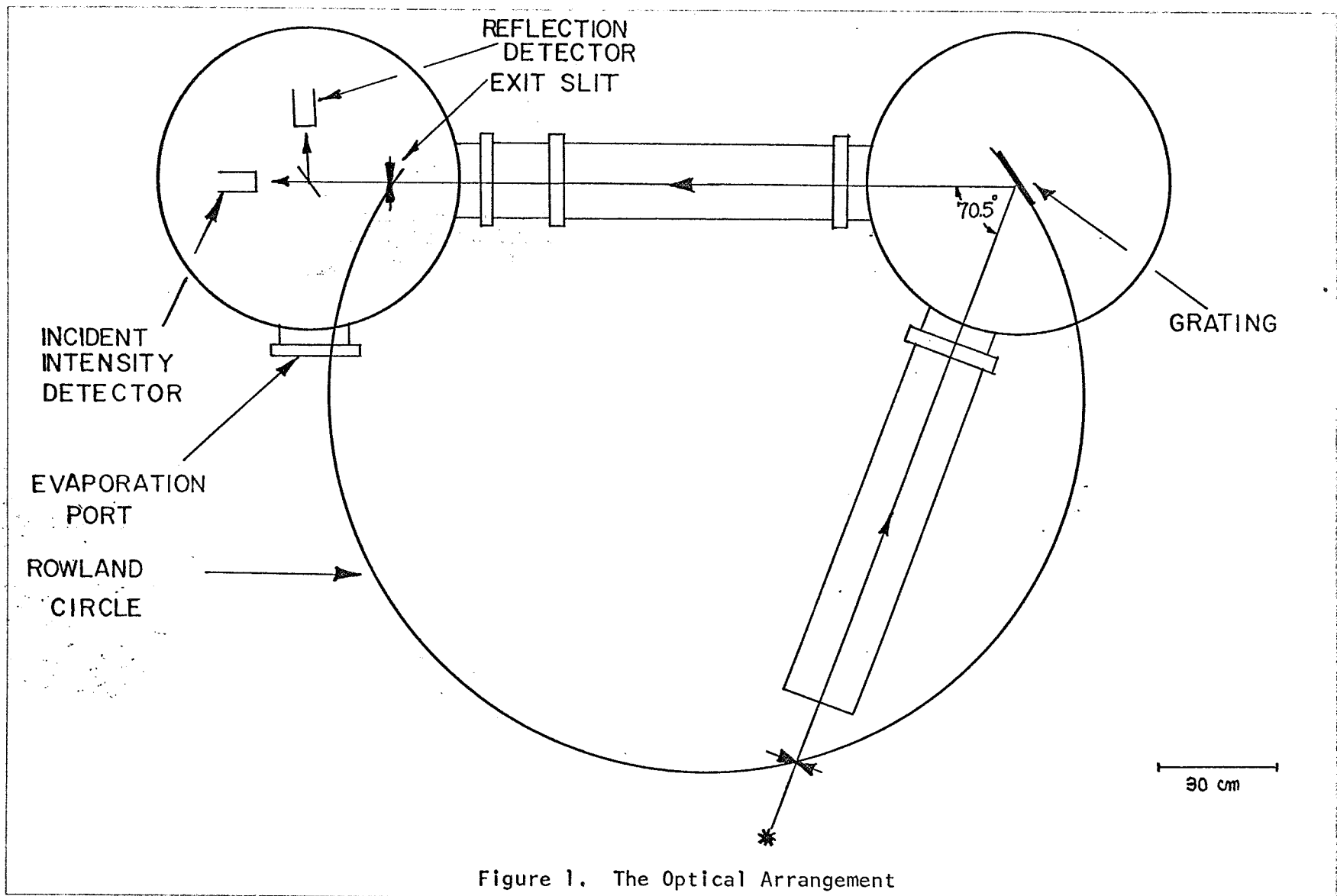
Since various materials will be studied, the best means of insuring a noncontaminated surface for all materials is to achieve an ultrahigh vacuum of the order of  $10^{-10}$  Torr, thereby assuring a monolayer time between 30 minutes and several hours depending on the sticking coefficient of the impinging contaminants.<sup>6</sup> It is the purpose of this work to describe the techniques which were used to attain a vacuum of this order and to discuss experiments in which this vacuum will be used.

## Experimental Apparatus

In order to determine experimentally the optical constants or the photoelectric yield of a material in the far uv, one must have a sufficiently intense uv source, a radiation disperser, a target and a detection system. Since reflection and photoelectric yield measurements are extremely sensitive to the condition of the surface which is to be studied, it is essential to have the target prepared and measured in an ultrahigh vacuum. This requirement, coupled with the lack of any adequate window material for far uv radiation, impels one to maintain all of the above components under conditions of an ultrahigh vacuum.

Radiation from the source (see Fig. 1) will pass through the entrance slit into an ultrahigh vacuum monochromator, be dispersed by a grating and focused on the exit slit of the monochromator. The angle between the entrance and exit arms of the monochromator is  $70.5^\circ$ , the Seya angle,<sup>7</sup> where defocusing is a minimum. The beam, after passing through the exit slit into the experimental chamber, impinges upon the target and is reflected to a detector.

The ultrahigh vacuum uv source must fulfill two requirements. It must not introduce a severe gas load into the system, yet it must produce sufficiently high uv intensity in the form of an emission continuum with superimposed lines. At present there are two such sources



available.<sup>8</sup> The first is a Q-switched laser which, when focused on a metallic target, creates a dense plasma fireball emitting radiation high in uv intensity. The second is a mechanically triggered vacuum spark between two metal electrodes. Both of these sources provide a high intensity continuum with superimposed lines in the uv and introduce only a very low gas load. Even with this low gas load induced by either of these sources, the entrance arm of the monochromator will be differentially pumped by a titanium getter on the source side of the entrance slit in order to reduce the amount of contaminants introduced into the system.

The radiation emitted by either of the above sources, after it passes through the entrance slit, will be dispersed by a 1m radius of curvature reflection grating, with 600 grooves per mm lightly ruled on glass, which is mounted inside the monochromator.

The monochromator chamber was constructed of type 304 stainless steel (see Fig. 2) and all welds were heliarced. This chamber was initially evacuated by a mechanical pump. A U-shaped trap was used between the mechanical pump and the fore-vacuum line in order to protect the system from pump oils. The second pump in the fore-line, a 700 l/sec oil diffusion pump, was separated from the primary 1400 l/sec diffusion pump by a liquid nitrogen cold finger trap. Pressure in the fore-line, measured by an ionization gauge, type VG1-A, attached between the cold finger trap and the 1400 l/sec oil diffusion pump, was usually between  $1 \times 10^{-6}$  and  $1 \times 10^{-7}$  Torr under normal operating conditions.

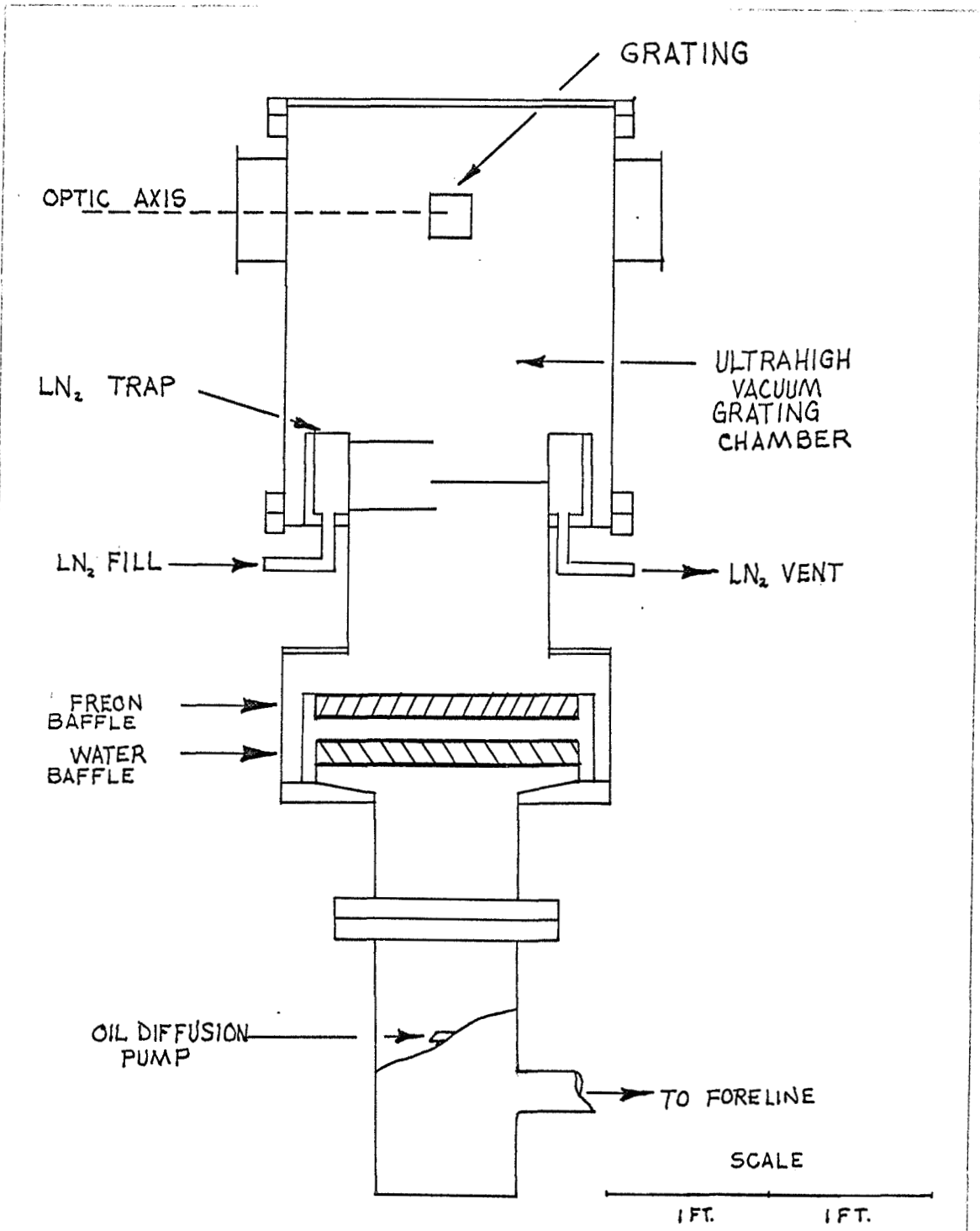


Figure 2. A Cross-Section of the Monochromator Vacuum System



The primary 1400 1/sec oil diffusion pump was separated from the monochromator chamber by a series of optically dense traps and baffles. The first was a water cooled baffle, the second a freon trap and the third a liquid nitrogen trap and baffle. These traps also prevented diffusion pump oil from migrating along the walls into the ultrahigh vacuum chamber and returned the oil to a cool part of the diffusion pump. The monochromator chamber, without the grating and with a titanium getter pump which deposited titanium onto the liquid nitrogen trap surface, consistently achieved a pressure of  $5 \times 10^{-10}$  Torr as measured by a nude Bayard-Alpert gauge. Despite the addition of the source and the grating this chamber should be capable of an operating pressure of the order of  $10^{-9}$  Torr.

The radiation that is dispersed by the grating travels down a windowless ultrahigh vacuum arm through a Whittaker\* isolation valve to the exit slit of the monochromator approximately 83 cm from the grating. The Whittaker valve, bakeable to  $400^{\circ}\text{C}$ , is used to isolate the monochromator from the reflectometer chamber so that either system may be let up to atmospheric pressure while the other may be maintained at ultrahigh vacuum. Each time it is necessary to open either the reflectometer or the monochromator, the respective system will be filled with dry nitrogen of 99.9% purity. This procedure will decrease contamination and allow access to the system several times in succession without necessitating a system bake-out in order to achieve an

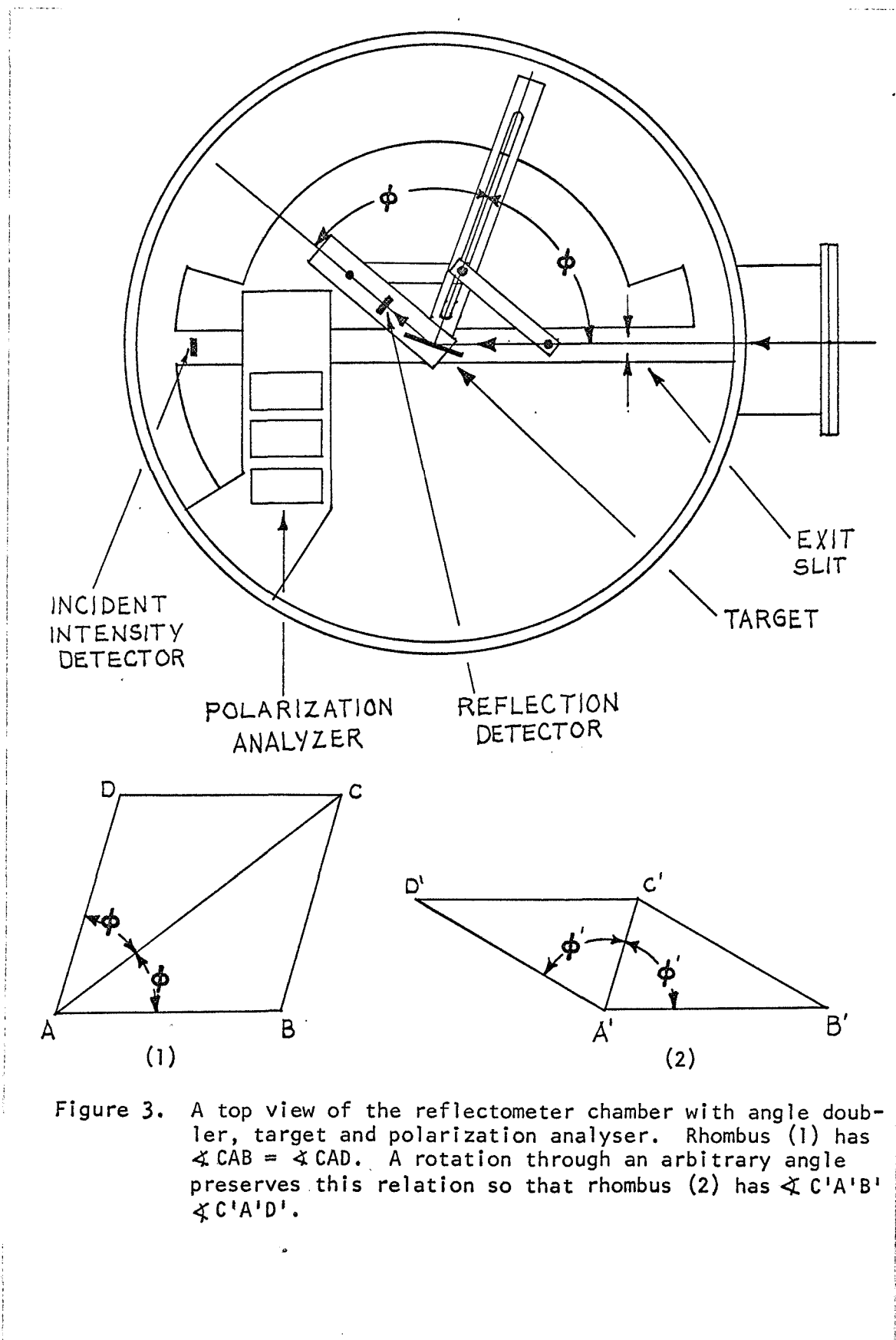
---

\*Whittaker Corporation, North Hollywood, California.

ultrahigh vacuum.

After the radiation passes through the exit slit, it will impinge upon the target and be reflected to a detector. An angle doubler (see Fig. 3) was constructed so that the angle between the optic axis and the target normal will be the same as the angle between the target normal and the detector axis. This apparatus was constructed of type 304 stainless steel and is mounted below the optic axis. It operates on the basic property of the rhombus. Its vertex (A) is positioned on the axis of rotation of the target. The diagonal (AC) is attached to the target so that it is always normal to the target surface. The arm (AB) of the rhombus is fixed parallel to the optic axis, while the arm (AD) is free to move and has the detector mounted on it. When the rhombus is deformed by rotation of the target, the angle CAB, the angle of incidence, will always equal the angle CAD so that the detector will intercept the reflected beam.

Since reflectances, the ratio of the reflected to incident intensity, will be used to determine the optical properties of the target material, there must be a detector to measure the incident beam and another to measure the reflected beam. The reflected and incident intensities should be measured simultaneously since nearly all vacuum uv sources produce radiation which varies in time. The target holder is constructed with horizontal slots so that part of the incident beam may pass through the target and be monitored by the incident intensity detector which is rigidly attached to its electrical feedthroughs on the optic axis behind the target.



The polarization analyser will also be mounted inside the reflectometer chamber. The apparatus, explained in greater detail in the chapter on Physical Measurements, consists of three separate stainless steel analysers, each containing four gold mirrors. This apparatus will normally be located off the optic axis as indicated in Fig. 3. During polarization measurements, the three analysers may individually be moved to a position directly behind the target substrate on the optic axis.

The target in the reflectometer chamber will be prepared by an evaporation of the sample material inside the experimental chamber onto the target holder. In order to decrease possible contamination, the sample material will be prepared according to the restrictions imposed by the sample material's chemical activity. If the sample material is extremely active, for example sodium, then it would be distilled in a vacuum system and while still under vacuum it would be sealed in a glass capsule. The capsule would then be placed in one of the evaporation elements and be introduced into the system for the experiment. Less active sample materials could be shaped and placed into the evaporator in an inert atmosphere and then introduced into the experimental system without fear of extensive contamination.

Once the sample material and evaporator have been placed into the system and a vacuum is achieved, the material should be out-gassed until there is almost no effect on the pressure when the amperage is increased to the threshold of evaporation. With a sample material such as sodium, it would, of course, be necessary to open the glass

capsule before the out-gassing could be accomplished.

After the material has been out-gassed, the target holder would then be rotated into position so that the normal to the target makes an angle of  $90^\circ$  with the incident optic axis in the plane of incidence and faces the evaporator. The material would then be deposited onto the holder. In order to keep the pressure of the system as low as possible, the titanium sublimator should be used throughout the evaporation period.

The present evaporator has six 200A ceramically insulated, electrical feedthroughs. With six feedthroughs the evaporator will accommodate two samples sealed in glass capsules, the other two feedthroughs would be used to open the glass capsules, or three samples in ordinary evaporation boats. The evaporation boats are made of tantalum sheet with a 0.005 inch wall thickness while the filament coils, which would hold the glass capsules, are made of  $3 \times 0.030$  inch multistrand tungsten wires. Alternatively, an electron beam evaporator may be used.

The evaporation unit will be encased in a copper shield in order to protect the reflectometer chamber from material evaporated into random directions. The sample material will be deposited on a glass substrate which will have been cleaned by acetone, xylene, ethanol and distilled water prior to being placed on the target holder.

The ultrahigh vacuum reflectometer tower, which contains the target, detectors, angle doubler and evaporation unit, was constructed of type 304 stainless steel using heliarc welding techniques. This

chamber (see Fig. 4) was evacuated first by Ultek\* sorption pumps at liquid nitrogen temperature in order to eliminate the possibility of introducing contaminating oil vapors into the system. After pressures of the order of 1 micron were reached the 400 l/sec ion pump was started. The fore-line was then closed off from the chamber by a Varian Associates\*\* isolation valve, bakeable to 350°C, capable of holding  $1 \times 10^{-11}$  Torr.

The Ultek ion pump<sup>9,10</sup> uses an electrical discharge in the presence of a strong magnetic field to sputter titanium from cathode plates. Active gases are removed from the system by ionization, dissociation and subsequent chemisorption on or in the sputtered titanium film. Inert gases are pumped by a mechanism called cathode burial.<sup>11,12</sup> In the cathode burial process the inert atoms are ionized and then accelerated to the cathode by the electrical field. On impact, they penetrate several atomic layers of the cathode and are occluded.

In addition to the ion pump, the reflectometer had a liquid nitrogen trap and baffle directly above the fore-line isolation valve and was equipped with a titanium getter pump. Pressure in this system was measured by a nude Bayard-Alpert gauge and the current of the ion pump.

---

\*Ultek Division, Perkin-Elmer, Palo Alto, California

\*\*Varian Associates, Palo Alto, California

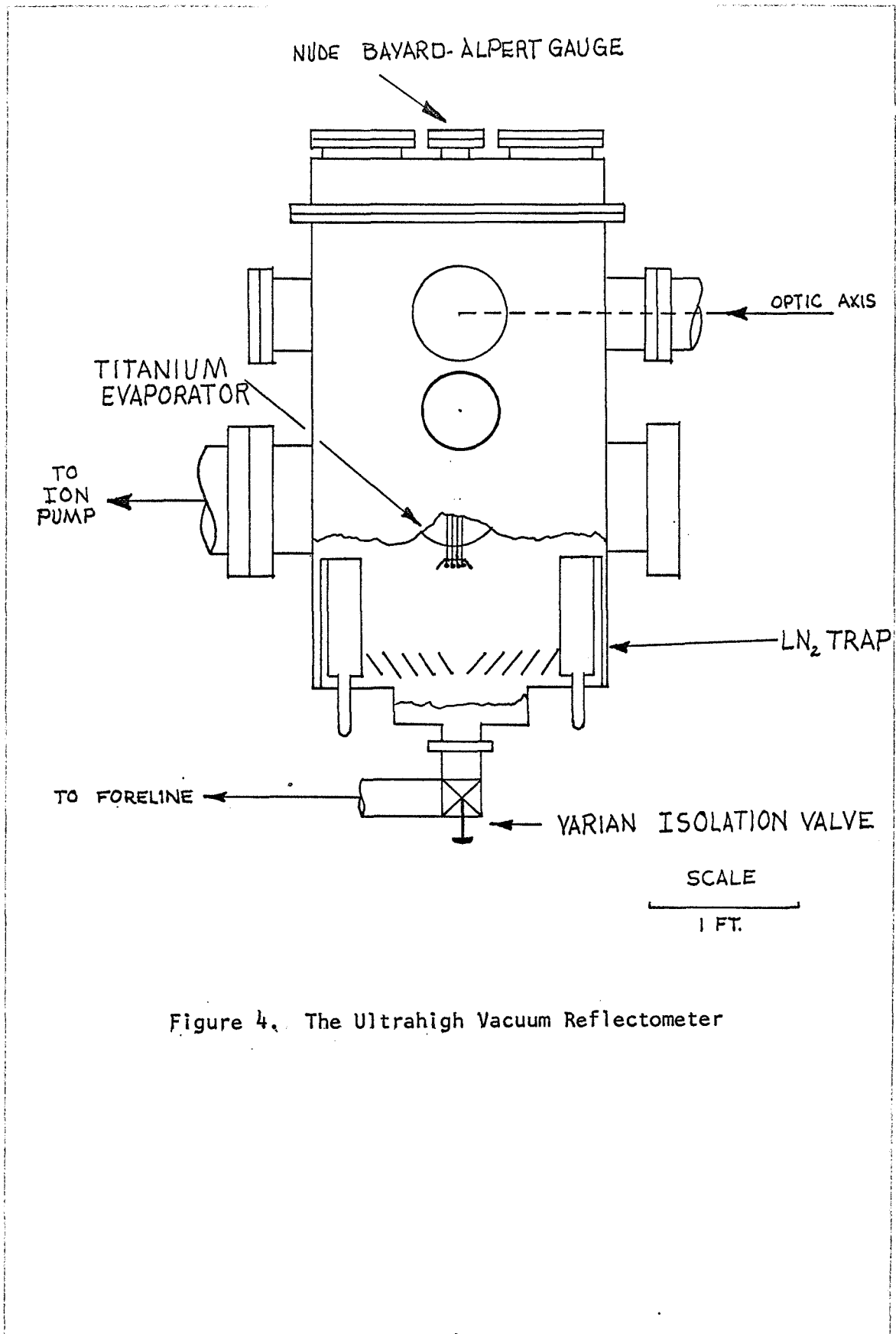


Figure 4. The Ultrahigh Vacuum Reflectometer

## Reflectometer Evacuation

In order to attain an ultrahigh vacuum it is necessary to limit the total leak rate and prevent contamination of the system. Both the monochromator and the reflectometer were leak tested with a mass spectrometer type helium leak detector manufactured by Consolidated Electro-dynamics Corporation.\* It was calibrated, prior to its use, by a standard helium leak and found to have a sensitivity of  $7 \times 10^{-11}$  standard cc/sec/division. In the case of the reflectometer, the leak detector was connected to the fore-line by tygon tubing with an O-ring seal. In an effort to prevent contamination by pump oils from the leak detector, the reflectometer chamber and the leak detector were separated by a liquid nitrogen trap, a molecular sieve and an isolation valve which was not opened until the actual leak testing was begun. The reflectometer was fore-pumped by the sorption pumps and the leak detector by its own mechanical pump. Once fore-pumped, the oil diffusion pump in the leak detector was turned on and allowed to heat up. The trap between the leak detector and the experimental system was then filled with liquid nitrogen after which the isolation valve between the detector and the reflectometer was opened.

---

\*Consolidated Electro-dynamics Corporation, Pasadena, California.



The area to be leak tested was then covered with a plastic bag and the natural helium background was measured. Helium was then introduced into the bag and the detector monitored for as long as two hours in order to obtain an accurate measurement. It was found necessary to place a fan near the bag so that the helium which did escape would not be introduced into the system through a leak in another location outside the bag. For a system with a 400 l/sec pump it is necessary to have a total leak rate on the order of  $10^{-8}$  Torr-l/sec in order to achieve a vacuum in the  $10^{-10}$  Torr range. The system was tested and repaired until the total leak rate was in this  $10^{-8}$  Torr-l/sec range.

Wherever possible, leaks that were found were repaired by replacing the appropriate components; however, if the leak was due to a faulty weld it was sometimes necessary to use a sealant such as Vacuum Leak Sealer made by the Vacuum Product Division of General Electric.\* This sealant, applied by a syringe, was used at the large 18 inch diameter double pinch seal of the reflectometer and appeared to seal effectively.

Once the leak rate was reduced to the low  $10^{-8}$  Torr-l/sec range, the system was baked-out over several periods of time totalling approximately 100 hours between temperatures of 150°C and 200°C. The low temperature bake-out was employed in order to prevent sealed leaks from re-opening and also to conform to the realistic limit imposed by the temperature sensitive emitter surfaces of the electron multipliers used

---

\*General Electric, Schenectady, New York.

for measuring radiation intensities. A bake-out in this temperature range served to drive surface contaminants, especially water vapor, from the walls of the system so they could be pumped out.<sup>13</sup> During bake-outs the ion pump was continually used, never allowing the pressure to exceed  $1 \times 10^{-5}$  Torr, so that the isolation valve between the experimental chamber and the fore-line could be kept closed and thereby prevent another possible means of contaminating the system.

After each bake-out of the chamber, the ion pump was baked out separately at  $150^{\circ}\text{C}$  until the pressure dropped into the  $10^{-8}$  Torr range. After several bake-out cycles, the system was allowed to return to its base pressure between  $3 \times 10^{-8}$  Torr and  $6 \times 10^{-9}$  Torr. The liquid nitrogen trap was filled and the nude Bayard-Alpert gauge out-gassed. After several minutes, the titanium sublimator was activated for a period of 45 seconds at a current of 45 A. The liquid nitrogen trap in conjunction with the titanium getter increased the pumping speed of the system by trapping molecules on the cold surface and chemically reacting with these contaminants. This procedure resulted in a reproducible pressure in the low  $10^{-10}$  Torr range as measured by the nude Bayard-Alpert gauge. A system pressure in this range assures one of a monolayer time comparable with the time required for an experiment approximately 30 minutes long. Pressures in this range were achieved without the sample or detectors and with the reflectometer chamber isolated from the monochromator on the reflectometer side by the Whittaker valve referred to earlier and shown in Fig. 1.

Numerous pumping cycles were performed with essentially the

same results: the nude Bayard-Alpert gauge ranging between  $1 \times 10^{-10}$  Torr and  $5 \times 10^{-10}$  Torr while the ion pump indicated a current between  $6 \mu\text{a}$  and  $10 \mu\text{a}$  which, according to Ultek, corresponds to a pressure range between  $1.0 \times 10^{-9}$  Torr and  $1.1 \times 10^{-9}$  Torr.

The ion current was plotted on a log-log graph against the nude Bayard-Alpert gauge pressure (Figs. 5 and 6). The correspondence, as exhibited on the Ultek calibration curve for the 400 l/sec ion pump, should be linear down to  $10^{-10}$  Torr. One can notice the relationship between the ion current and the nude Bayard-Alpert gauge above  $2 \times 10^{-9}$  Torr is linear and almost in exact correspondence with the predicted curve. The range below  $2 \times 10^{-9}$  Torr shows a different behavior. The ion current approaches a lower limit of six or seven micro amps.

There are several phenomena which may cause this discrepancy. The first is the possible contamination of the ion pump. The accessible surfaces of the pump were cleaned with acetone and ethanol. However, surfaces which were inaccessible, and therefore not cleaned, admit numerous possibilities for virtual leaks. The second is the so-called argon memory or argon instability,<sup>14</sup> in which the impact of inert gas ions on the cathode causes a re-emission of previously pumped ions which show up as an increase in the ion current. The last is that in the process of sputtering, small amounts of titanium were deposited on the surfaces of some of the ceramic insulators in the ion pump, thereby creating conducting paths which would show up as an increase in the minimum, or base, current achievable. The last phenomena would indicate a pressure in the ion pump higher than in the system and set a

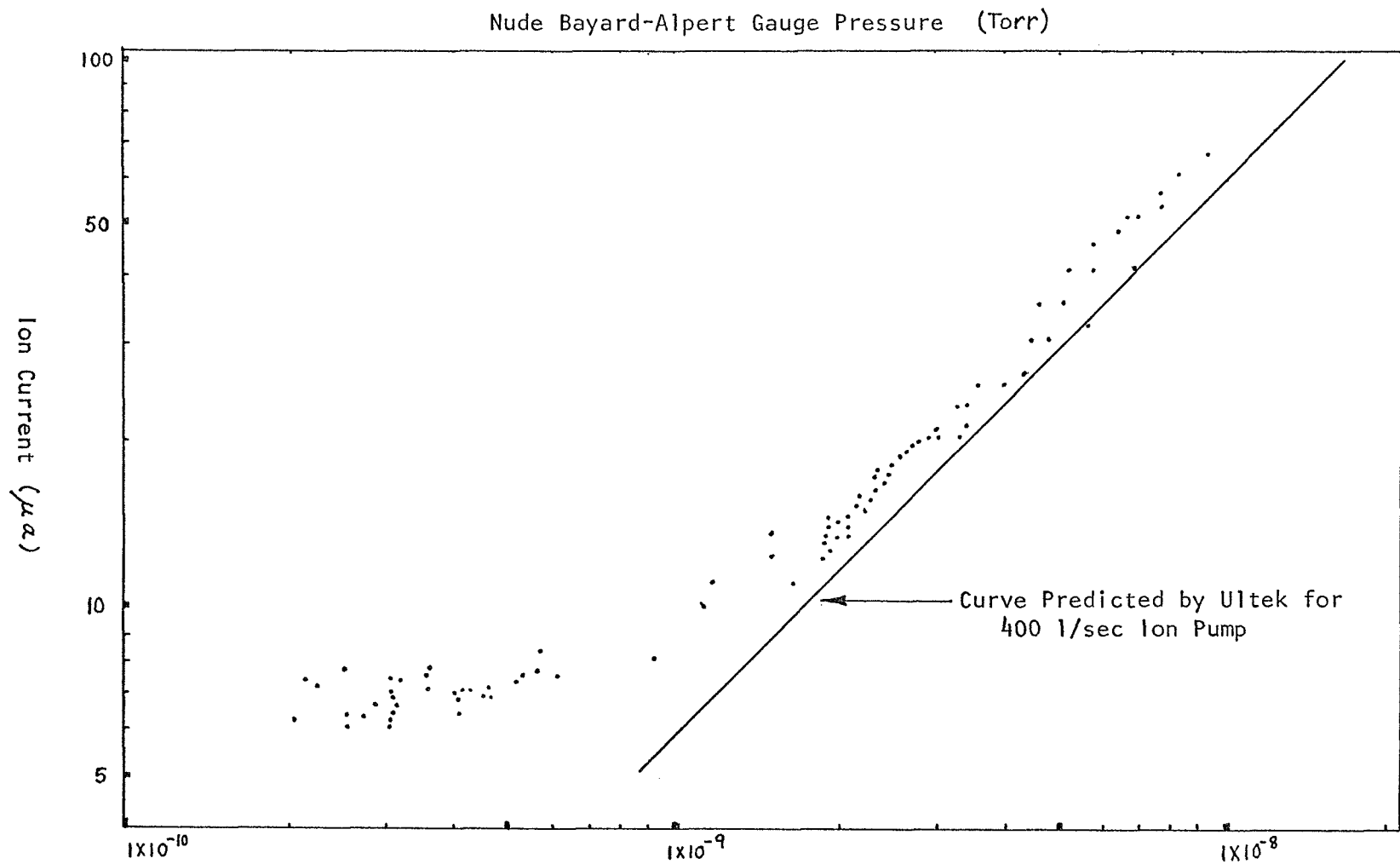


Figure 5. Ion pump current plotted against Nude Bayard Alpert gauge pressure for a composite of pumping cycles

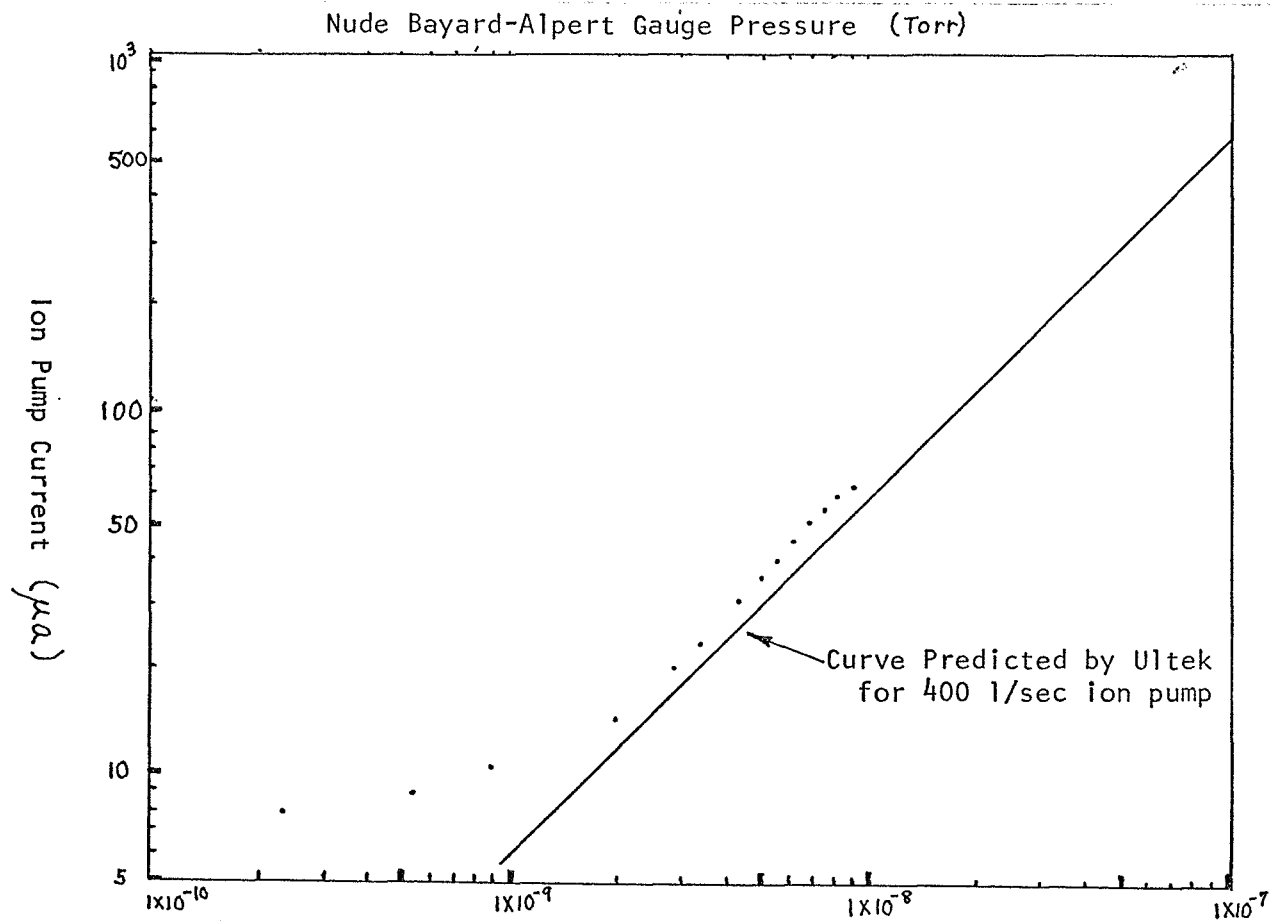


Figure 6. Ion pump current for one pump down cycle plotted against the Nude Bayard-Alpert gauge pressure.

constant lower limit to the measurable ion current.

In both the reflectometer and the monochromator chambers, wherever possible, oxygen free high conductivity, OFHC, gaskets were used in conjunction with a single or double pinch seal.<sup>15</sup> Other materials and types of seals were used whenever it was necessary to conform with those used in commercially produced apparatus. The ion pump required Curvac\* seals, the nude Bayard-Alpert gauge used a gold O-ring and the 1400 l/sec oil diffusion pump employed an aluminum gasket.

---

\*Curvac Seal manufactured by Ultek Division of Perkin-Elmer, Palo Alto, California.

## Physical Measurements

Once a satisfactory vacuum has been achieved, the target material may be deposited on to the target substrate, and after evaporation, the system will quickly return to its base pressure. Reflectance measurements may then be taken after the polarization has been determined. The procedure will involve a measurement over the desired spectral region for various incident angles between normal and grazing. The reflected and incident intensities will be simultaneously measured by two electron multipliers. The purpose of multiple measurements is to supply other check points at each wavelength. When using nomograms\* to reduce data, large errors can be introduced from some portions of the nomograms (an error of  $\pm 1\%$  in both reflectance values can produce an accuracy of only about  $\pm 5\%$  in the values of  $n, k$ ).<sup>16</sup> This error is caused by having the lines of constant  $n$  and the lines of constant  $k$ , for two particular angles of incidence, be so close to one another that a slight variation in the reflectances will cause a large error in the optical constants.

Since a small error in the reflectance, defined as the reflected intensity divided by the incident intensity, can cause a large error in

---

\*Curves of constant  $n$  and constant  $k$  plotted in the  $R(\theta_1), R(\theta_2)$  plane, where  $\theta_1$  and  $\theta_2$  are different angles of incidence.

the optical constants, and since either the vacuum spark or laser generated fireball produce large intensity variations between consecutive light pulses, the incident and reflected intensities must be measured for each pulse, which may be accomplished by beam splitting.<sup>17</sup> Some experimenters have used a sodium salicylate coated mesh between the exit slit and the target in conjunction with a second photomultiplier looking at the mesh. However, in order to increase the flexibility of this apparatus the target will be constructed with four horizontal slits (see Fig. 7). These slits will enable sampling of the beam at different heights by the incident intensity electron multiplier located behind the target and on the optic axis.

In order to determine the reflectance, the reflected intensity from the target and the intensity incident upon it must be known. The ratio of the measured incident intensity, that which passes through the target, to the actual incident intensity, that which impinges upon the target surface, will depend only upon the geometry of the target. Once this ratio has been determined, one may measure the intensity of the beam which passes through the target and then divide by the constant ratio to determine the incident intensity which is to be used in calculating the reflectance.

This ratio will be determined by first measuring  $I_0$ , the intensity from a stable source with the target moved up and out of the optical path,  $I_0'$ , the fraction of the incident intensity which passes through the target when it is in its normal position on the optic axis. The actual incident intensity,  $I_0''$ , which impinges upon the target will



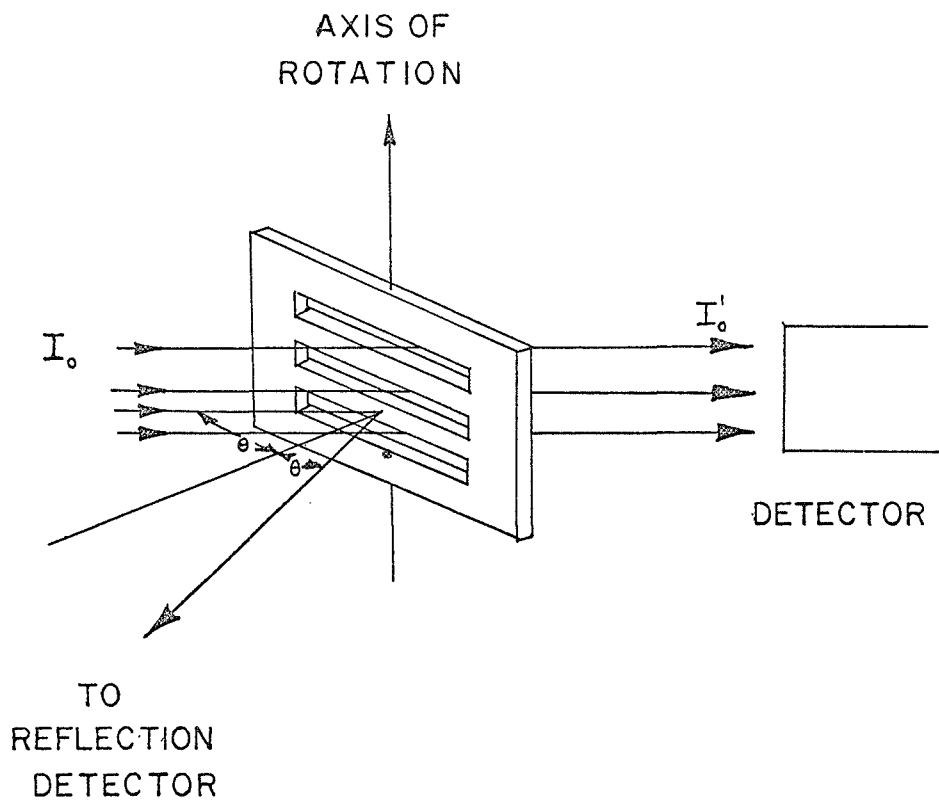


Figure 7. Target with Slots for Determining Incident Intensity

then be

$$I_0'' = I_0 - I_0'$$

so that the required constant ratio is

$$C = \frac{I_0''}{I_0'} = \frac{I_0 - I_0'}{I_0'}$$

During an experiment  $I_0'$  and  $I_R$ , the reflected intensity, will be measured. The reflectance,  $R$ , will then be calculated as:

$$R = \frac{I_R}{I_0''} = \frac{I_R}{I_0' C}$$

The next phase of the experiment will be to determine the polarization of the radiation incident upon the target. The polarization is defined as

$$P = \frac{I_p - I_s}{I_p + I_s},$$

where  $s$  and  $p$  refer to the intensity components normal and parallel to the plane of incidence, respectively. This, along with the reflectance data at each wave length, is needed to solve the Fresnel equations for the optical constants.

There are several reflection techniques<sup>18,19,20</sup> for determining polarization in the far uv, all involving a different number of measurements or a different number of reflections. In our case, determining the polarization will involve three separate measurements each with four reflections, a modification of a method developed by A.L. Morse<sup>20</sup> at this laboratory and subsequently used at Desy in

Hamburg.<sup>21</sup> It is believed that the source will be sufficiently intense to make such measurements possible. The polarization analyser consists of four gold mirrors such that the angle of incidence on each of the mirrors will be about  $60^\circ$  (see Fig. 8).

This method will involve first a measurement  $I_1$ , with the four mirrors of the analyser and grating having a common plane of incidence. The second measurement,  $I_2$ , will have the planes of incidence of the four mirrors of the analyser perpendicular to the plane of incidence of the grating. The third measurement,  $I_3$ , will have the plane of incidence of the grating parallel to the planes of incidence of the first two mirrors of the analyser and perpendicular to the planes of incidence of the second two mirrors of the analyser.

With light of intensity  $I_0$  and unknown polarization coming from the grating and incident on the analyser, the measured intensities are given by the relationships

$$I_1 = I_s r_s^4 + I_p r_p^4,$$

$$I_2 = I_s r_p^4 + I_p r_s^4,$$

$$I_3 = I_s r_s^2 r_p^2 + I_p r_p^2 r_s^2,$$

where  $I_s$  and  $I_p$  are the perpendicular and parallel components of the intensity of the beam after it passes through the exit slit and  $r_s$  and  $r_p$  are the perpendicular and parallel reflectances of each of the gold mirrors of the analyser respectively. It has been assumed that  $r_s$  and  $r_p$  are the same for each of the mirrors of the analyser.

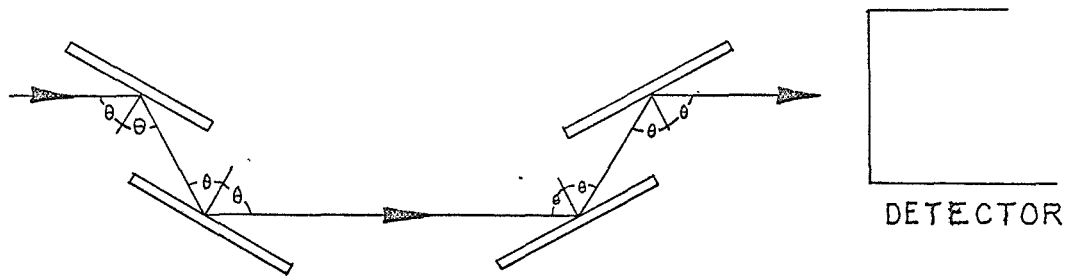


Figure 8. The four gold mirrors of the polarization analyser are shown in a position to measure  $I_1$ , yielding transmitted light with the E-vector mostly perpendicular to the plane of the paper. The angle of incidence  $\theta$  is  $60^\circ$  on each of the mirrors. This system can be rotated by  $90^\circ$  about the optic axis in order to transmit mostly plane polarized light with the E-vector parallel to the plane of the paper.

Defining the quantities

$$A = \frac{I_p}{I_s},$$

$$B = \frac{r_p^2}{r_s^2},$$

and

$$C = I_s r_s^4,$$

then the measured intensities take the form

$$I_1 = C(1 + AB^2),$$

$$I_2 = C(B^2 + A),$$

$$I_3 = C(B + AB).$$

The ratio  $A$  is found to be

$$A = \Gamma - \sqrt{\Gamma^2 - 1},$$

where

$$2\Gamma = \frac{I_1^2 + I_2^2 - 2I_3^2}{I_1 I_2 - I_3^2}.$$

The polarization is then calculated from the expression

$$P = \frac{A - 1}{A + 1}.$$

In solving these equations we have assumed that for a given wavelength the quantity  $C$  is the same for all measurements. Since it does involve the incident intensity, special attention must be given

to light source fluctuations. For each measurement at a given wavelength the incident radiation can be normalized, thereby making  $C$  a constant for that wavelength. This can be accomplished by intercepting the beam with a slotted target holder (at a fixed orientation) such that part of the beam is reflected to an electron multiplier and the remaining fraction is transmitted to the analyser. This reflected beam intensity provides a means of monitoring the fluctuations of the light source. By dividing the reflected beam's signal into that of the transmitted beam the normalization is achieved.

There is considerable evidence<sup>15</sup> that the polarization is dependent upon the surface conditions of the grating. This dependence can either be attributed to a chemical change in the surface, such as oxidation, causing a change in the optical constants of the grating or to physical adsorption of contaminants. Since a glass grating will be used in the proposed experiment, the chemical effect should become negligible leaving adsorption of contaminants as the primary cause. The degree of contamination may depend upon the pressure in the monochromator and the prior history of cleaning of the grating. For this reason, the monochromator will be maintained at a vacuum of about  $10^{-9}$  Torr when the polarization of the exit beam is measured.

## Summary and Conclusion

In preparation for experiments which will determine the optical constants and energy-loss functions of various solids, an ultrahigh vacuum chamber was constructed and tested. The requirements for this system were to achieve a vacuum on the order of  $10^{-10}$  Torr and to eliminate as many sources of surface contamination as possible.

Such sources of contamination are best eliminated by choosing the proper materials for construction and making the appropriate selection of pumps. This system was constructed of stainless steel type 304 with all heliarc welding and all of the gaskets were made of OFHC copper. The sorption type fore-pumps used no oil and therefore eliminated one of the serious sources of contamination present in conventional vacuum systems. Following along similar lines, a liquid nitrogen cold trap in conjunction with a titanium sublimator and an ion pump were chosen because their pumping action did not introduce contaminants.

A reproducible vacuum of the desired order was achieved after bake-out followed by periodic use of the titanium sublimator in conjunction with the cold trap. The pressure of the system was monitored by a nude Bayard-Alpert gauge and continually indicated a reading in the  $10^{-10}$  Torr range.

#### List of References

1. J.C. Phillips, Phys. Rev. 133, A452 (1964).
2. R. Tousey, J. Op. Soc. Am. 29, 235 (1939).
3. W.R. Hunter, J. Op. Soc. Am. 55, 1197 (1965).
4. H. Fröhlich and H. Pelzer, Proc. Phys. Soc. (Lond.) A68, 525, (1955).
5. H. Kanazawa, Prog. Theoret. Phys. (Kyoto) 26, 851 (1961).
6. R.W. Roberts and T.A. Vanderslice, Ultra High Vacuum and Its Applications (Prentice Hall, Inc., Englewood Cliffs, New Jersey, 1963), p. 3.
7. M. Seya, Sci. Light (Tokyo) 2, 8 (1952).
8. N. Wainfan and J.E. Rudisill, A Vacuum Spark Light Source for the Extreme Ultra Violet Region (Technical Report No. USC-Vac. UV-111, Prepared for NASA), July 15, 1968.
9. T. Tom and B.D. James, Inert Gas Ion Pumping Using Differential Sputter Yield Cathodes (Ultek Corporation) Reprint from 13th National Vacuum Symposium of the American Vacuum Society, October 26-28, 1966.
10. L.D. Hall, Rev. Sci. Instr. 29, 367 (1958).
11. K. Kamasaki et. al., J. Appl. Phys. 35, 470 (1964).
12. J.M. Lafferty and T.A. Vanderslice, Proc. I.R.E. 49, 1136 (1961).



13. R.W. Roberts and T.A. Vanderslice, Ultra High Vacuum and Its Applications (Prentice Hall, Inc., Englewood Cliffs, New Jersey, 1963), p. 123.
14. R.W. Roberts and T.A. Vanderslice, Ultra High Vacuum and Its Applications (Prentice Hall, Inc., Englewood Cliffs, New Jersey, 1963), p. 21-24.
15. W. Steinmann, E.I. Fisher and G.L. Weissler, Optical Constants of Metals in the Vacuum Ultraviolet Regions (Technical Report Prepared for NASA) , January 15, 1964.
16. E.I. Fisher, I. Fujita, and G.L. Weissler, J. Op. Soc. Am. 56, 1560 (1966); see also Optical Constants of Silver and Barium in the Vacuum Ultraviolet Spectral Region (Technical Report No. USC-Vac. UV-108, Prepared for NASA), May 1, 1966.
17. R.W. Ditchburn, J. Quant, Spectr. Radiative Transfer 2, 361 (1962).
18. K. Rabinovitch, L.R. Canfield, R.P. Madden, Appl. Opt. 4, 1005 (1965).
19. R.N. Hamm, R.A. MacRae, E.T. Arakawa, J. Op. Soc. Am. 55, 1460 (1965).
20. A.L. Morse, Optical and Photoelectric Properties, Including Polarization Effects of Gold and Aluminum in the Extreme Ultra Violet (Technical Report No. USC-Vac. UV-109, Prepared for NASA) January 5, 1968.
21. M. Skibowski, B. Feuerbacher, R. Godwin and W. Steinman, Z. Phys. 211, 329 (1968).